

Molecular Promoting of Aluminum Metal–Organic Framework Topology MIL-101 by *N,N*-Dimethylformamide

Maarten G. Goesten,^{*,†} Pieter C. M. M. Magusin,[‡] Evgeny A. Pidko,^{*,§} Brahim Mezari,[§] Emiel J. M. Hensen,[§] Freek Kapteijn,[†] and Jorge Gascon^{*,†}

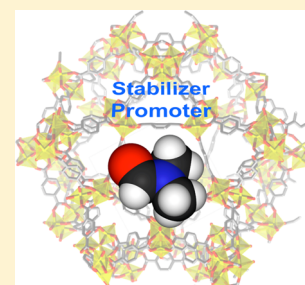
[†]Catalysis Engineering, Delft University of Technology, Julianalaan 136, 2628 BL Delft, The Netherlands

[‡]Centre for Surface Science and Catalysis, KU Leuven, Kasteelpark Arenberg 23 - bus 2461, 3001 Leuven, Belgium

[§]Schuit Institute of Catalysis, Eindhoven University of Technology, P.O. Box 513, 5600MB Eindhoven, The Netherlands

Supporting Information

ABSTRACT: In situ NMR and DFT modeling demonstrate that *N,N*-dimethylformamide (DMF) promotes the formation of metal–organic framework NH₂–MIL-101(Al). In situ NMR studies show that upon dissociation of an aluminum-coordinated aqua ligand in NH₂–MOF-235(Al), DMF forms a H–Cl–DMF complex during synthesis. This reaction induces a transformation from the MOF-235 topology into the MIL-101 topology. Electronic structure density functional theory (DFT) calculations show that the use of DMF instead of water as the synthesis solvent decreases the energy gap between the kinetically favored MIL-101 and thermodynamically favored MIL-53 products. DMF therefore promotes MIL-101 topology both kinetically and thermodynamically.



INTRODUCTION

Much of the chemistry that governs the early processes in crystallization of metal–organic frameworks (MOFs) is complex and still not known in detail.¹ This hampers the prediction of novel materials with targeted applications. Revealing the crystallization mechanism can result in optimized syntheses and may also deliver more general information on MOF crystallization.²

Recent work of our group in this field mainly focused on two MOF topologies, MIL-53 and MIL-101.^{3–6} The advantage of choosing the MIL-53 and MIL-101 topologies as model systems is 3-fold: (i) Their thermal and chemical stability make them frontrunners among MOF materials of industrial interest.⁷ (ii) They are made from identical precursors yet form under very different conditions. (iii) They can be synthesized for different metals and different ligands. In this case, aminated ligands are used as they provide readily solubilized linkers, which facilitate in situ spectroscopic studies with multiple solvents.^{8–10}

In investigating the competition between formation of the thermodynamically favored phase NH₂–MIL-53(Al) and kinetic phase NH₂–MIL-101(Al), we relied on small- and wide-angle X-ray scattering (SAXS/WAXS) to unravel the kinetics and mechanistic pathways of crystallization.⁸ An important observation was that the use of the metal chloride precursor in DMF as (co)solvent led to the presence of an intermediate structure, NH₂–MOF-235(Al), for which analogous species were earlier found during the crystallization of iron carboxylates.^{11,12} Depending on the solvent, this intermediate can convert either into NH₂–MIL-53(Al) or NH₂–MIL-101(Al). The use of DMF–H₂O solvent mixtures in the synthesis of NH₂–MIL-53(Al) leads to significantly improved

material yield compared to the synthesis in pure H₂O.¹³ The use of pure DMF as solvent sees NH₂–MOF-235(Al) transforming into NH₂–MIL-101(Al). Chemically, this transformation only matters with the change of one terminal ligand per three alumina and elimination of charge-balancing AlCl₄[−], as shown in Figure 1.

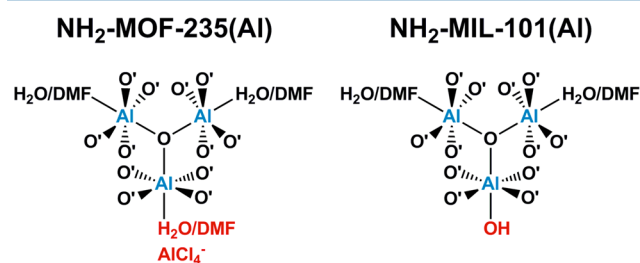


Figure 1. Simplified representation of the μ_3 -O-centered cluster that builds NH₂–MOF-235 and NH₂–MIL-101. The 12 oxygen ligands denoted by O' originate from the μ_4 -2-aminoterephthalato ligands, which are not further displayed for the sake of clarity.

Despite these findings, the seemingly promotional role of DMF and its interplay with AlCl₃·6H₂O has remained unclear. In order to resolve these obscurities, we decided to carry out a study at the molecular level, using in situ ¹H and ²⁷Al NMR in combination with DFT. We will show in this work that the role of the DMF in synthesis is surprisingly versatile; apart from acting as the solvent, it is directly involved in promoting

Received: August 28, 2013

Published: January 9, 2014

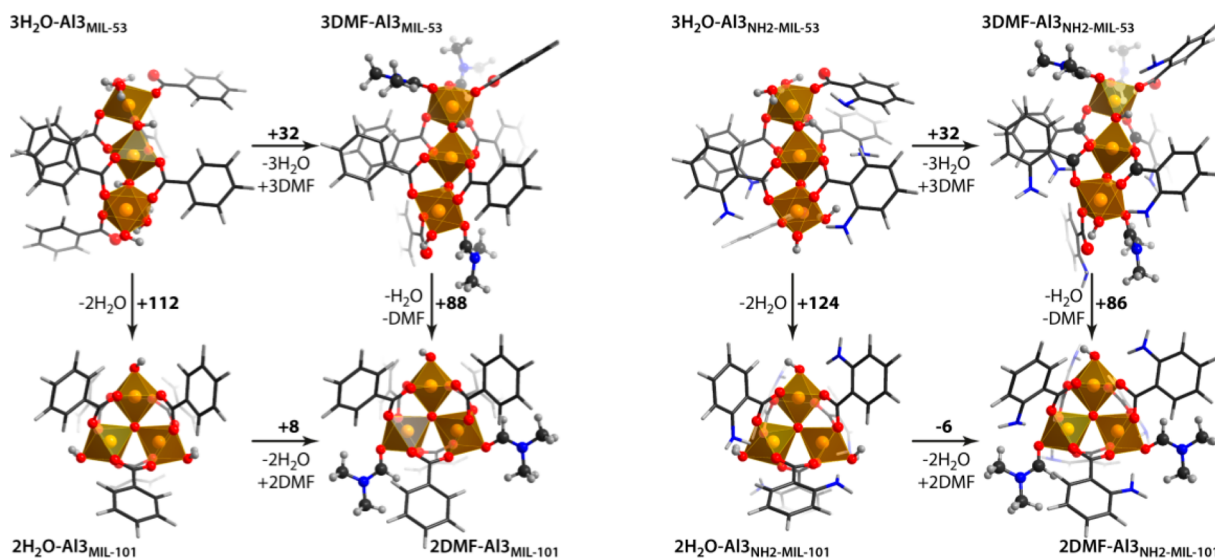


Figure 2. Solvent–ligand-induced transformations of trinuclear Al clusters representing structure-forming units of MIL-53 and MIL-101 topologies. DFT-computed reaction energies are given in kJ/mol above the arrows indicating respective chemical transformations. Left: MIL-53(Al) and MIL-101(Al). Right: NH₂–MIL-53(Al) and NH₂–MIL-101(Al).

formation of MIL-101(Al) both thermodynamically and kinetically.

EXPERIMENTAL SECTION

In Situ NMR Experiments. In situ NMR spectra were recorded on a Bruker DRX200 spectrometer, operating at ¹H and ²⁷Al NMR frequency of 200 and 52 MHz, respectively. The NMR experiment is in essence a liquid-state experiment, but in order to extend the NMR detectability of larger chemical structures in confined space (such as Al–DMF complexes) that are normally beyond the typical limits of detection in solution NMR, the synthesis solutions were rotated under the magic angle at a sample rotation rate of 1.1 kHz. For these magic angle spinning (MAS) experiments a Bruker 7 mm MAS WVT (wide variable temperature) probe head with temperature was used. The temperature was controlled via a temperature controller placed close the sample. Control proceeds using a heated and cooled nitrogen flow. The temperature controller was calibrated using the melting of polyethylene glycol (61 °C). To contain the pressure buildup at 130 °C, specially designed home-constructed PEEK (polyether ether ketone) inserts with screwable caps were used inside the standard zirconia 7 mm MAS rotors. This PEEK insert was filled with the precursor solution for NH₂–MIL-101(Al), which was prepared in the following way. In one beaker, 0.507 g of AlCl₃·6H₂O was mixed with 15 mL of (dried) DMF; in another beaker, 0.564 g of 2-aminoterephthalic acid was mixed with in 15 mL of DMF. Both solutions were stirred ultrasonically and then mixed and quickly loaded into the insert.

¹H and ²⁷Al MAS NMR spectra were recorded in an alternating way in the course of time. For ¹H NMR spectra, the number of scans was 16, and the relaxation delay between the scans was 10 s. For ²⁷Al NMR spectra, the number of accumulated scans was 256, and the relaxation delay was 1 s.

DFT Calculations. Similar to our previous study,¹⁴ density functional theory (DFT) was performed with the meta-GGA M06 L exchange-correlation functional by Zhao and Truhlar¹⁵ and a full electron 6-31G(d,p) basis set. All calculations were performed with the Gaussian 09 software.¹⁶ The initial structures of MOF precursors were constructed by cutting an appropriate charge-neutral structural motif containing three Al centers from crystal structures of MIL-53 and MIL-101.

Terephthalate and amino-terephthalate ligands were simplified with benzoate and meta-amino benzoate ligands. The octahedral coordina-

tion of Al centers in the models was ensured by introducing H₂O or DMF ligands at the unsaturated sites.

RESULTS

In computationally examining the stabilizing role of DMF on the μ₃-O-centered cluster, we built four representative clusters of MIL-53(Al), MIL-101(Al), NH₂–MIL-53(Al), and NH₂–MIL-101(Al). Each cluster contains three aluminum centers and coordinated benzoic and 2-aminobenzoic acid mimic terephthalic acid and 2-aminoterephthalic acid, respectively. The results of DFT calculations (Figure 2) are in good agreement with experimental observations as they indicate that MIL-53(Al) is the thermodynamically preferred topology in both H₂O and DMF, but stabilization of the linear Al₃ MIL-53 cluster is more pronounced in water. Exchanging the aqua ligands for DMF ligands leads to an increase in energy of 32 kJ/mol. This energy increase is smaller in the case of the μ₃-O-centered Al₃ MIL-101 cluster, 8 kJ/mol, but enough to obstruct formation of MIL-101(Al), which has not been isolated in literature yet at the time of writing. When the amino-functionalized carboxylic acid is considered as the ligand, energetics of the ligand exchange for the MIL-53 clusters remain effectively unchanged (ΔE = +31 kJ/mol), depicted in Figure 2 at the right. However, the exchange of two aqua ligands in the μ₃-O-centered Al₃ NH₂–MIL-101(Al) cluster for two DMF molecules becomes exothermic (ΔE = –6 kJ/mol). The origin of this small but important stabilization is not clear at the time of writing.

We thus see that the combination of DMF and the aminated ligand stabilizes the μ₃-O-centered cluster of NH₂–MOF-235(Al) and NH₂–MIL-101(Al), yet it does not explain the transition of the former phase into the latter. We performed an in situ NMR study in order to demystify this.

It was not up until very recently that in situ NMR was used to study the crystallization of metal–organic frameworks. Haouas et al. demonstrated the existence of several intermediate solid phases during the syntheses of aluminum trimesates MIL-96, MIL-100, and MIL-110 and proposed corresponding reaction pathways.¹⁷ In situ NMR is a most powerful tool for the study of small complexes; it can reveal the

subtle changes in coordination chemistry around the metal ion during MOF synthesis and is able to clearly identify previously unknown chemical events and/or structures.¹⁸

In the current case, we must first note that delocalization of the lone-pair electrons in the DMF molecule does not only cause it to preferentially coordinate via its oxygen atom, it also causes the two methyl groups to be chemically nonequivalent, and six signals corresponding to coordinated and uncoordinated DMF are observed in a ¹H NMR experiment of a DMF/AlCl₃·6H₂O solution at room temperature (Supporting Information).¹⁹ The NH₂-MIL-101(Al) precursor solution shows these six peaks next to a broad water peak, originating from the metal chloride hydrate, as well as small peaks in the aromatic region that belong to the 2-aminoterephthalic acid linker.

Figure 3 shows the temperature-controlled in situ ¹H spectra of the precursor solution as it is heated to the MOF synthesis

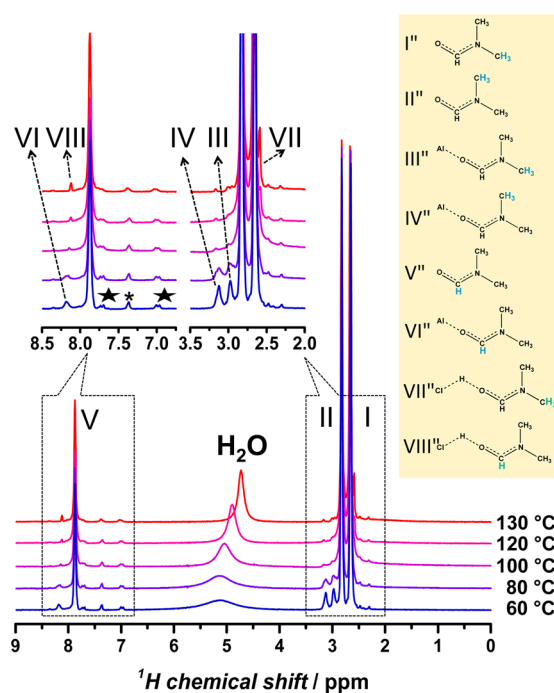


Figure 3. Temperature-programmed in situ ¹H NMR spectra of NH₂-MIL-101(Al) synthesis. Species are identified in the legend on the right, ★ marks peaks of dissolved 2-aminoterephthalic acid, and * marks a ¹³C-¹H satellite.

temperature of 130 °C. A first observation is that the three signals corresponding to DMF coordinated to aluminum vanish as the complex dissociates, and aluminum is left free for coordination to the MOF linker. Linker signals disappear concurrently as the framework crystallizes, and the linker is consumed from the solution. The water signal is seen to shift to a higher field and sharpens strongly during this process. This combination of line sharpening and shift to higher field is a normal observation during the heating of water. It is caused by the weakening of the hydrogen-bonding interactions during the heating process. Protons are as a result more effectively shielded from the magnetic field, causing the upfield shift, with better defined electron density, causing the sharper resonance.²⁰ An interesting observation is the appearance of two extra visible proton resonances, suggesting the presence of a previously unknown moiety in solution (VII and VIII, Figure

3).²¹ Because of the use of AlCl₃·6H₂O, we suspected this moiety to be a H-Cl-DMF complex; in the literature, this is described as a highly stable species that readily forms in HCl-DMF mixtures.²²

We carried out additional ¹H NMR experiments on DMF-HCl mixtures to confirm that the additional peaks are indeed caused by this complex (Supporting Information). Figure 4

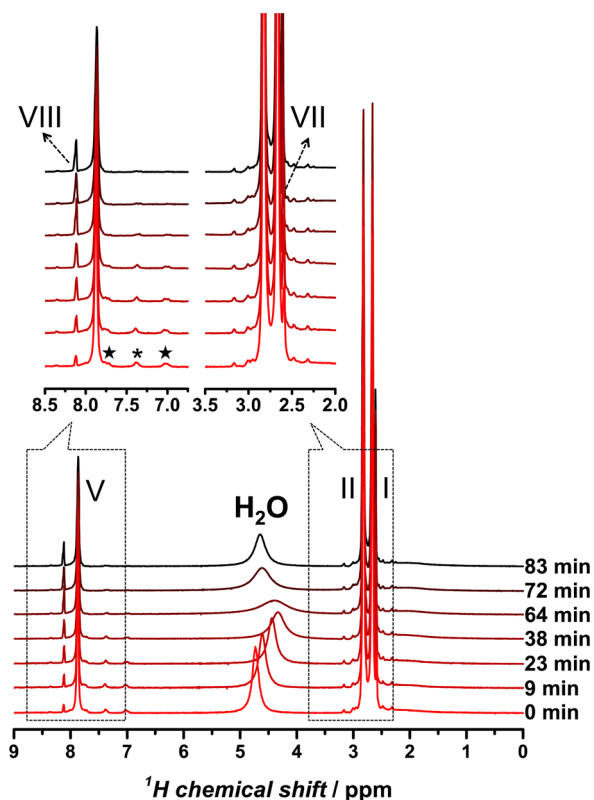


Figure 4. In situ ¹H NMR spectra of NH₂-MIL-101(Al) synthesis at 130 °C, following up on Figure 3.

displays the time-resolved development at 130 °C for which we know NH₂-MOF-235(Al) forms almost instantaneously, and NH₂-MIL-101(Al) forms after approximately 25–30 min. One can first of all see that the concentration of the H-Cl-DMF complex increases rapidly as the solution is kept at 130 °C.

Further, the water signal undergoes several changes. At the early stages at 130 °C, we see that the water signal keeps moving upfield long after the synthesis temperature of 130 °C had been reached. We attribute this effect to the “consumption” of water in solution. Water dissociates into protons, and the μ₃-O ligands that make up the NH₂-MOF-235(Al) framework/integration of the water signal confirms that over the whole time-space, 16% of water is lost, which lies within the expected range of 11–28%.²³ A lower concentration of water in DMF leads to less pronounced hydrogen bonding between water molecules and a shift to higher fields. Interestingly, after approximately 30 min, the reverse phenomenon is visible; the water signal broadens, indicating rapid exchange, and promptly shifts to a lower field. This remarkable “shifting” of the water signal was a fully reproducible observation that we could rationalize with the help of DFT. We propose that the very stable H-Cl-DMF complex *molecularly promotes* the formation of NH₂-MIL-101(Al). It does so by providing the required hydroxido ligand, which distinguishes NH₂-MIL-101(Al) from

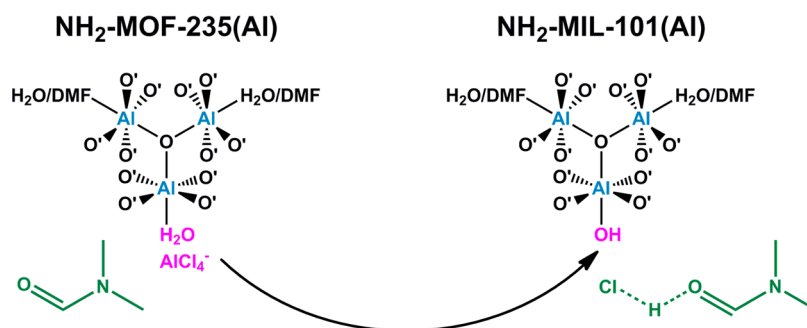


Figure 5. Promoting effect of DMF in formation of $\text{NH}_2\text{-MIL-101(Al)}$. AlCl_3 dissociates and is rapidly taken up in the new framework.

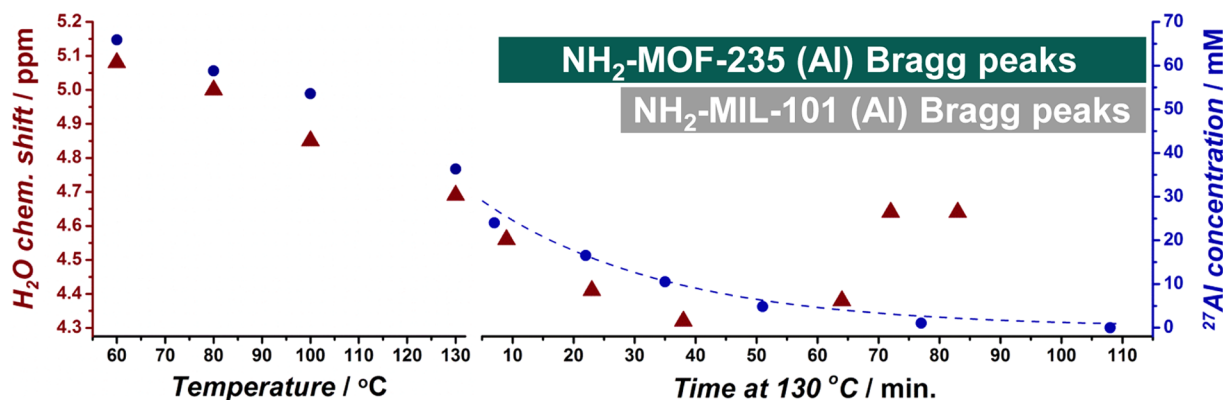


Figure 6. H_2O chemical shift (dots, blue) and aluminum concentration (pyramids, red) as a function of temperature during temperature-ramping (left) and as a function of time at $130\text{ }^\circ\text{C}$ (right). The time domains of crystalline $\text{NH}_2\text{-MOF-235(Al)}$ and $\text{NH}_2\text{-MIL-101(Al)}$ are also indicated. Aluminum concentration profile at $130\text{ }^\circ\text{C}$ is fitted for a first-order reaction with $k = 0.033\text{ (s}^{-1}\text{)}$.

$\text{NH}_2\text{-MOF-235(Al)}$ (Figure 1), through a water dissociative mechanism. This reaction would lead to a sudden increase in the concentration of solvated protons, which would explain the observed exchange line broadening as well as the “acidic” downfield shift of the water signal. Such a reaction is normally highly unfavorable, and our DFT study indeed indicated that such a reaction of the form $\text{Cl}^- + \text{H}_2\text{O} + \text{DMF} \rightarrow \text{OH}^- + \text{H-Cl-DMF}$ is strongly endothermic ($+272\text{ kJ/mol}$) due to the insufficient stabilization of the hydroxide anions. However, when considering the exchange of Cl^- by the OH^- anion in the coordination sphere of the Al^{3+} center, which would be the case in a $\text{NH}_2\text{-MOF-235(Al)}$ to $\text{NH}_2\text{-MIL-101(Al)}$ rearrangement, energetics are much more favorable ($+2\text{ kJ/mol}$). $\text{NH}_2\text{-MIL-101(Al)}$ is expected to be the entropically and thermodynamically preferred lattice as the noncoordinate charge separation is eliminated, and this is likely to be the driving force behind the observed transition.

We can thus with confidence state that DMF acts as a molecular promoter, providing required hydroxido ligands to selectively form the kinetic MIL-101 phase (Figure 5).

Finally, we carried out the same *in situ* NMR experiment but for the ^{27}Al nucleus. The ^{27}Al spectrum displays one peak, corresponding to dissolved octahedrally coordinated Al^{3+} , which decays in time as aluminum is consumed during crystallization of the framework (Supporting Information).

We calculated the concentration of Al^{3+} in solution in time, which is displayed in Figure 6, along with the chemical shift of H_2O . During temperature ramping, aluminum is consumed in the formation of larger structures that are not crystalline yet. This can be concluded from the fact that no Bragg peaks are observed in this time domain of crystallization, and structures

apparently carry enough chemical shift anisotropy to prevent peaks in liquid-state NMR experiments. From $130\text{ }^\circ\text{C}$ onward, Al^{3+} concentration decays steadily. The trend resembles the one of a reactant concentration decaying in a first-order reaction, and we fitted this correspondingly, though rather to provide a guide to the eye than a kinetic rationale. An important result is that the trend is maintained throughout the remainder of the synthesis, including the time domain where $\text{NH}_2\text{-MOF-235(Al)}$ rearranges into $\text{NH}_2\text{-MIL-101(Al)}$.

DISCUSSION AND CONCLUSIONS

Summarizing, we demonstrate that the combination of the amine functionality in 2-aminoterephthalic acid and DMF stabilizes the formation of the $\mu_3\text{-O}$ -centered cluster that builds $\text{NH}_2\text{-MOF-235(Al)}$ and $\text{NH}_2\text{-MIL-101(Al)}$. Furthermore, the role of DMF is very versatile as *in situ* ^1H NMR shows that upon dissociation of an aluminum-coordinated aqua ligand in $\text{NH}_2\text{-MOF-235(Al)}$ DMF forms a H-Cl-DMF complex during synthesis. The formation of this complex induces a transformation from the MOF-235 topology into the MIL-101 topology because it leaves a terminal hydroxido ligand. This ligand is required for formation of MIL-101. We thus see that a combination of the metal *chloride* precursor and DMF are required for successful synthesis of $\text{NH}_2\text{-MIL-101(Al)}$, which fits laboratory observation.

The physical transformation of $\text{NH}_2\text{-MOF-235(Al)}$ into $\text{NH}_2\text{-MIL-101(Al)}$ is an interesting point. In the preceding work, using *in situ* small-angle X-ray scattering, we observed that the transformation from $\text{NH}_2\text{-MOF-235(Al)}$ into $\text{NH}_2\text{-MIL-101(Al)}$ proceeds without any change in morphology or size of the crystals.¹⁰ As we now see from NMR experiments,

the aluminum concentration decays steadily over the whole time domain, and a reaction between a terminal aqua ligand and DMF in the aluminum coordination sphere induces the transformation. We conclude that the hypothesis of a dissolution–recrystallization mechanism predominating as suggested earlier by us should be rejected (although a solid-to-solid rearrangement will involve interaction with the solvent).⁸ The transformation of NH₂–MOF-235(Al) into NH₂–MIL-101(Al) thus occurs in the solid state and is induced by the reaction displayed in Figure 5. Similar types of solid-state transformations have been reported in MOF literature before²⁴ and owe their existence to MOFs being coordination compounds, in which a process of dative bond breakage and reformation is continuously present.²⁵ This phenomenon has been associated to the large crystallinity of MOFs in general²⁶ but also provides the possibility of solvent-assisted ligand exchange,²⁷ and here, topologic transformations occur within the solid state.

NH₂–MIL-53(Al) was earlier identified as the thermodynamic product of the synthesis mixture and is seen to be the only product in syntheses over much longer periods of time. The promoting role of DMF also affects NH₂–MIL-53(Al) synthesis, which is evident from the observation that already small (10%) additions of DMF to the H₂O synthesis mixture of NH₂–MIL-53(Al) yield a 3-fold increase of the latter.⁸ The isolated Al–(μ_2 -OH) chains are more efficiently obtained when there is a hydroxido ligand-generating solvent like DMF, yet the solvent is not required to obtain the framework. For NH₂–MIL-101(Al) synthesis, DMF can be seen as an indispensable moiety, which is required to promote the kinetic product.

It is possible that similar solvent-promotional effects can also be observed with other widely used chemicals such as DMSO, which is, among others, also known to form complexes with HCl. A last but important remark is that this work deals with aluminum-based MOFs, and this chemistry is not necessarily to be extrapolated to MOFs based on transition metals. Haouas et al. but also Ribas in his textbook on coordination chemistry discussed how similar μ_3 -O-based building blocks form easily (ergo, early in synthesis) for *d*-metals, but assembly is more complicated when dealing with aluminum (*p*-block) chemistry.^{17,28} That said, aluminum MOFs are among the most interesting materials due to stability and catalytic inertness from an application point of view, which makes the study on their formation significant. In conclusion, we have shown how the choice of an appropriate solvent can lead to specific MOF topologies and/or large improvements in yield by acting as a versatile promoter in MOF synthesis while demonstrating the power of in situ NMR to unravel underlying molecular mechanisms. Yield and topology dependence on solvents has been commonly observed by other groups, but to our knowledge, these are barely explained at the molecular scale. The information presented in this work may allow the synthesis of new MOF topologies and/or higher yields of existing ones.

■ ASSOCIATED CONTENT

■ Supporting Information

¹H NMR analysis on DMF/HCl mixtures and DMF/AlCl₃·6H₂O mixtures, in situ ²⁷Al NMR spectra, and XRD patterns. This material is available free of charge via the Internet at <http://pubs.acs.org>.

■ AUTHOR INFORMATION

Corresponding Authors

*E-mail: M.G.Goesten@tudelft.nl (M.G.G.).

*E-mail: E.A.Pidko@tue.nl (E.A.P.).

*E-mail: J.Gascon@tudelft.nl (J.G.).

Notes

The authors declare no competing financial interest.

■ ACKNOWLEDGMENTS

Technology Foundation STW, The Netherlands, and Hyflux CEPAration Technologies Europe BV are gratefully acknowledged for financial support through the partnership program STW-Hyflux CEPAration Inorganic and Hybrid membranes. Part of the research leading to these results has received funding (J.G.) from the European Research Council under the European Union's Seventh Framework Programme (FP/2007-2013)/ERC Grant Agreement n. 335746, CrystEng-MOF-MMM. We thank Dr. Kristina Djanashvili for additional ¹H NMR experiments on the H–Cl–DMF mixtures.

■ REFERENCES

- (1) Goesten, M. G.; Kapteijn, F.; Gascon, J. *CrystEngComm* **2013**, *15*, 9249–9257.
- (2) Stock, N.; Biswas, S. *Chem Rev* **2012**, *112*, 933–969.
- (3) Serra-Crespo, P.; Stavitski, E.; Kapteijn, F.; Gascon, J. *RSC Adv* **2012**, *2*, 5051–5053.
- (4) Serra-Crespo, P.; Gobechiya, E.; Ramos-Fernandez, E. V.; Juan-Alcañiz, J.; Martinez-Joaristi, A.; Stavitski, E.; Kirschhock, C. E. A.; Martens, J. A.; Kapteijn, F.; Gascon, J. *Langmuir* **2012**, *28*, 12916–12922.
- (5) Serra-Crespo, P.; van der Veen, M. A.; Gobechiya, E.; Houthoofd, K.; Filinchuk, Y.; Kirschhock, C. E. A.; Martens, J. A.; Sels, B. F.; De Vos, D. E.; Kapteijn, F.; Gascon, J. *J. Am. Chem. Soc.* **2012**, *134*, 8314–8317.
- (6) Serra-Crespo, P.; Ramos-Fernandez, E. V.; Gascon, J.; Kapteijn, F. *Chem. Mater.* **2011**, *23*, 2565–2572.
- (7) Schubert, M.; Mueller, U.; Kiener, C. Aluminium Amino-carboxylates as Porous Metal Organic Frameworks. US8313559 B2, 2012
- (8) Stavitski, E.; Goesten, M. G.; Juan-Alcañiz, J.; Martinez-Joaristi, A.; Serra-Crespo, P.; Petukhov, A. V.; Gascon, J.; Kapteijn, F. *Angew. Chem., Int. Ed.* **2011**, *50*, 9624–9628.
- (9) Juan-Alcañiz, J.; Goesten, M. G.; Martinez-Joaristi, A.; Stavitski, E.; Petukhov, A. V.; Gascon, J.; Kapteijn, F. *Chem Commun* **2011**, *47*, 8578–8580.
- (10) Goesten, M. G.; Stavitski, E.; Juan-Alcañiz, J.; Martinez-Joaristi, A.; Petukhov, A. V.; Kapteijn, F.; Gascon, J. *Catal. Today* **2013**, *205*, 120–127.
- (11) Sudik, A. C.; Cote, A. P.; Yaghi, O. M. *Inorg. Chem.* **2005**, *44*, 2998–3000.
- (12) Millange, F.; Medina, M. I.; Guillou, N.; Ferey, G.; Golden, K. M.; Walton, R. I. *Angew. Chem., Int. Ed.* **2010**, *49*, 763–766.
- (13) The observation that DMF–H₂O mixtures lead to improved yields inspired us to find an optimal solvent composition for the synthesis of NH₂–MIL-53(Al). We found that a composition of DMF:H₂O of 0.1:0.9 leads to a 300% improvement in yield with respect to pure water synthesis.
- (14) van den Bergh, J.; Gucuyener, C.; Pidko, E. A.; Hensen, E. J. M.; Gascon, J.; Kapteijn, F. *Chem.—Eur. J.* **2011**, *17*, 8832–8840.
- (15) Zhao, Y.; Truhlar, D. G. *J. Chem. Phys.* **2006**, *125*, 194101.
- (16) Frisch, M. J. et al. *Gaussian 09*, Revision B.01; Gaussian, Inc., Wallingford, CT, 2009.
- (17) Haouas, M.; Volklinger, C.; Loiseau, T.; Ferey, G.; Taulelle, F. *Chem. Mater.* **2012**, *24*, 2462–2471.

(18) Houssin, C. J. Y.; Kirschhock, C. E. A.; Magusin, P. C. M. M.; Mojet, B. L.; Grobet, P. J.; Jacobs, P. A.; Martens, J. A.; Van Santen, R. A. *Phys. Chem. Chem. Phys.* **2003**, *5*, 3518–3524.

(19) Emons, H. H.; Siedler, M.; Thomas, B.; Porzel, A. *Z. Anorg. Allg. Chem.* **1988**, *558*, 231–239.

(20) Hartel, A. J.; Lankhorst, P. P.; Altona, C. *Eur. J. Biochem.* **1982**, *129*, 343–357.

(21) For the reader wondering where the other methyl proton signal and H–Cl proton signal are in the spectra, we suspect the first one is overlapped by the intense methyl proton signal of the uncoordinated solvent, and the H–Cl proton signal is invisible due to rapid exchange.

(22) Kislina, I. S.; Librovich, N. B.; Maiorov, V. D.; Tarakanova, E. G.; Yukhnevich, G. V. *Kinet. Catal.* **2002**, *43*, 671–674.

(23) This range is spanned by the terminal aqua ligand parameter. When looking at Figure 1, the minimum assumes that zero terminal (solvent) ligands of the μ_3 -O cluster are aqua; ergo all consumed water goes to the μ_3 -O ligand. The maximum assumes two terminal ligands of the trigonal cluster are aqua. These extremes correspond to 11.11% and 27.80%, respectively, and the reality lies somewhere in the middle, as confirmed by NMR experiments. We can conclude from the integration that every trigonal cluster has on average 0.58 aqua ligands and 1.42 DMF ligands in this synthesis.

(24) Min, K. S.; Suh, M. P. *J. Am. Chem. Soc.* **2000**, *122*, 6834–6840.

(25) Bernini, M. C.; Gándara, F.; Iglesias, M.; Snejko, N.; Gutiérrez-Puebla, E.; Brusau, E. V.; Narda, G. E.; Monge, M. Á. *Chem.—Eur. J.* **2009**, *15*, 4896–4905.

(26) Beaudoin, D.; Maris, T.; Wuest, J. D. *Nature Chem.* **2013**, *5*, 830–834.

(27) Li, T.; Kozłowski, M. T.; Doud, E. A.; Blakely, M. N.; Rosi, N. L. *J. Am. Chem. Soc.* **2013**, *135*, 11688–11691.

(28) Ribas Gispert, J. *Coordination Chemistry*, 1st ed; Wiley-VCH Verlag: Weinheim, Germany, 2008.